*GEOLOGICA CARPATHICA, 44, 4, BRATISLAVA, AUGUST 1993*
*219 - 232*

# PRESSURE-TEMPERATURE CONDITIONS OF METAMORPHISM IN THE NORTHERN PART OF THE BRANISKO CRYSTALLINE COMPLEX

ANNA VOZÁROVÁ

Geological Institute of Dionýz Štúr, Mlynská dolina 1, 814 07 Bratislava, Slovak Republik

*(Manuscript received February 22, 1991; accepted in revised form March 31, 1993)*

**Abstract:** Relics of the HT/HP events have been identified in the gneiss-amphibolite complex of northern part of the Branisko Mts. The assemblage Grt + Bt + Kfs + Pl ± Sil ± Ky is characteristic of the gneisses and migmatites. The methods of Grt + Bt thermometry and Grt + Bt + Pl + Sil barometry were used for the determination of temperature and pressure. P-T conditions at the boundary of granulite facies were calculated from almandine cores with high pyrope component contents ($X^{Gt}_{Mg}$ = 0.19 - 0.27) and biotite ($X^{Bi}_{Mg}$= 0.4 - 0.6) in the temperature range 675 - 770 °C and pressure range 400 - 630 MPa. A regressive P-T trend was detected in garnet rims. The calculated regression temperatures and pressures are in the range of 590 - 648 °C and 300 - 400 MPa, respectively.
The regression trend represents probably a compression and depression phase of the same metamorphic event. The pre-Permian age of the event is evidenced by the occurrence of pebbles of the gneiss-migmatite complex in Permian conglomerates. A more precise age determination (Variscan or pre-Variscan stage) is not possible owing to lacking geochronological data. Another retrograde alterations are related to hydrothermal-metasomatic processes and cataclastic deformations both in late-Variscan (blastomylonite and cataclasite pebbles in Permian) and Alpine stage.

**Key words:** granulite facies relics, geothermometry, geobarometry, Branisko Mts., Western Carpathians.

## Introduction

The crystalline complex of northern part of the Branisko Mts. consists of high grade metamorphic rocks, gneisses and migmatites. Chemical compositions of critical mineral phases in gneisses and migmatites were determined by means of electron microprobe in order to derive P-T conditions of metamorphism. Several calibrations of garnet-biotite thermometer (Ferry & Spear 1978; Hodges & Spear 1982; Perchuk et al. 1983; Ganguly & Saxena 1984; Indares & Martignole 1985) were used for the calculations. The methods were discussed with respect to their suitability for individual samples and selection was made for mean statistical data.

A basis for the pressure calculations were phase relations in the assemblage garnet - biotite - plagioclas - sillimanite and/or kyanite. Mean statistical pressure values were calculated using calibrations of Newton & Haselton (1981), Koziol & Newton (1988) and Powell & Holland (1988). A program written by M. Janák (Department of Mineralogy and Petrology, Comenius University) and P. Pitoňák (Geological Institute, Slovak Academy of Sciences) was used for thermo- and barometry calculations.

All mineral analyses were performed using the electron microanalyser "Superprobe" (JCXA-733) in the Geological Institute of Dionýz Štúr in Bratislava.

## Geological structure

The northern part of the Branisko Mts. is built up by the crystalline massif of Patria, Upper Paleozoic and Mesozoic cover rocks and of upper nappes (Fig. 1). Mesozoic sequences of central and northern Branisko Mts. comprise the Krížna Nappe (Fusán et al. 1963; Maheľ in Maheľ et al. 1967) and in the Lačnová dolina Valley also the Triassic of the Choč Nappe (Rösing 1947; Polák 1987). To the north of the Branisko saddle Upper Paleozoic rocks were distinguished and correlated with the Nižná Boca and Malužiná Forms. of Hronic Nappes (The geologic and paleogeographic map of Carboniferous and Permian of Czechoslovakia - Holub & Vozár et al. 1981; Vozárová & Vozár 1986, 1988).

The crystalline massif of Patria (the northern Branisko) consists of biotite, and garnet-biotite, gneisses intimately connected with the complex of anatectic migmatites and magmatites which form a substantial part of the massif. Amphibolite bodies and amphibole gneisses form a part of the complex. The metamorphic and magmatic rocks of the massif of Patria along with their Permian and Mesozoic cover form a tectonic unit in the Branisko Mts. which was always correlated with Tatric units (Rösing 1947; Kamenický in Fusán et al. 1963; Andrusov 1958; Maheľ et al. 1967; Maheľ 1986).

However, on the basis of lithology, metamorphic degree and character of magmatic members, the crystalline complex, together with Permian - Mesozoic cover, resembles rather the northern Veporic units. Recently, Vozárová & Vozár (1986) correlated the complex with this unit. The authors compare the complex with analogical sequences in the Starohorské vrchy Hills. Besides the crystalline rocks, a strong similarity exists between the lithology of Upper Paleozoic (Korytné *vs.* Špania dolina Valley Forms. - Vozárová & Vozár 1986, 1988) and Mesozoic. The Lower Triassic sequences, largely reduced in the Branisko Mts., are lithologically identical with the Lužná Beds described by Fejdiová (1980). Similarly as in the northern Veporicum (Horehron Valley, Čierťaž, Starohorské vrchy Hills)

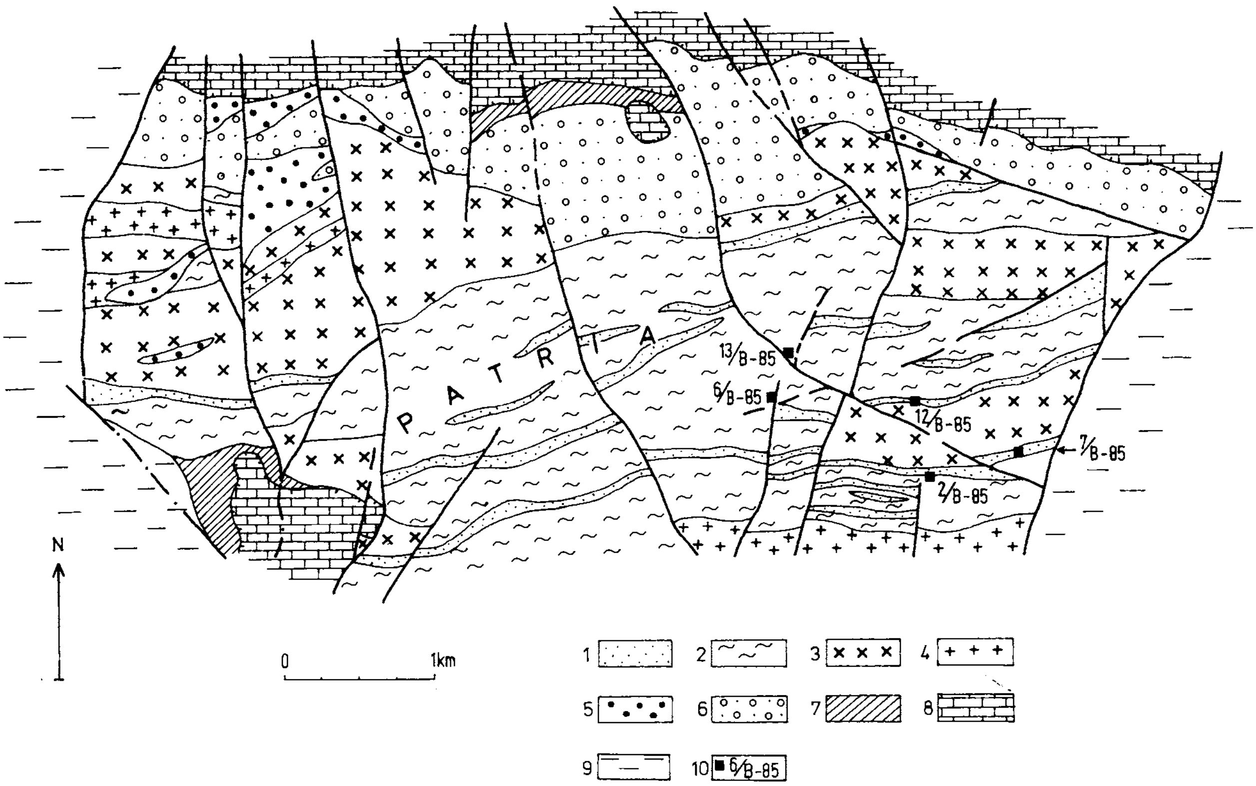


**Fig. 1.** Geological map of the northern Branisko Mts.: the massif of Patria (Vozár in Polák et al. 1985).
*Legend:* 1 - garnet-biotite gneisses; 2 - migmatites; 3 - medium-grained granitoids (granodiorites and tonalites); 4 - fine-grained leucogranite; 5 - Permian: Korytné Formation (conglomerates, rarely sandstones and shales); 6 - Lower Triassic: sandy shales, carbonates, dolomites; 8 - Hronicum: the Šturec Nappe as the whole; 9 - Paleogene sediments; 10 - sample localization.

also in the Branisko exists the same superposition relation of the Križna Nappe. The nappe occurs in this rear part in the position of multiple folded cover directly underlying the upper tectonic unit, the Šturec Nappe (Polák 1987; Vozárová & Vozár 1986, 1988).

## Characterization of crystalline rocks

The northern Branisko complex of high grade metamorphic rocks is formed by garnet-biotite gneisses, migmatites, and less frequent amphibole gneisses and amphibolites.

The gneisses are greyish, of massive or banded fabric, mostly strongly foliated and fine-grained. The equigranular texture is formed by the mosaic of xenoblastic grains of quartz and feldspars the intergranular space being filled up by short laths of biotite and rarely amphibole. Modal compositions of analysed samples is given in Tab. 1. Prevailing phases of gneisses are plagioclases (30 - 40 vol. %) and quartz (30 vol. %). Primary muscovite is not a member of the association. The plagioclase, being rarely antiperthitic, has composition of oligoclase. Often perthitic alkali feldspar is orthoclase (max. 10 vol. %). The coexisting critical mineral association is represented by biotite and garnet rarely accompanied by sillimanite (A'FM diagram, Fig. 2) or relict kyanite. The relics of platy quartz are common in the rock structure.

Based on the structural relations, kyanite, very rarely occurring with sillimanite, is an unstable relict being replaced by long, prismatic sillimanite structurally markedly oriented together with biotite. The garnet content in gneisses ranges between 3 - 6 vol. %, the biotite content around 25 vol. %. Aluminosilicates occur in gneisses generally in low quantities which is probably a result of primary source lithology and partially a result of later, regressive, alterations, mainly by replacing of aluminosilicates by muscovite.

The critical mineral association Grt + Alm + Sil + Ky is characteristic also of migmatites. Migmatites have massive banded, or schlieren fabric with macroscopically markedly distinguished bands or irregular pools of neosom. The neosom is mainly of leucocratic (Qz + Pl + Kfs) composition with low biotite content. In melanocratic parts of the neosom the biotite content increases being associated with sillimanite, garnet or amphibole. Rarely, the diablastic structures have formed, composed of Grt + Bt + Qz + Kfs. The texture of migmatites is typically heterogeneous exhibiting the alternation of relatively more coarse-grained bands with non-oriented, or weakly oriented, minerals and finer grained bands with distinctly oriented grains of biotite, quartz and plagioclase. Feldspars form irregular elongated porfyroblasts or grains tending to prisms. Rarely, such grains are enclosed in fine-grained quartz aggregate. Plagioclases tend to be zoned (more basic cores are entirely altered). The subhedral plagioclases commonly occur in finer-grained, relatively equigranular parts of rock. Compared with the gneisses described above the contents of quartz and plagioclase increase moderately and contents of mafic minerals, biotite and garnet, decrease.

**Table 1:** Modal mineral composition of analysed samples.

| | 7/B-85 | 12/B-85 | 2/B-85 | 6/B-85 | 13/B-85 |
|---|---|---|---|---|---|
| Quartz | 30.5 | 27 | 32 | 32 | 29 |
| Plagioclase | 27.5 | 28 | 31 | 33 | 38 |
| Orthoclase | 7.0 | 16 | 10 | 9 | 17 |
| Biotite | 29.0 | 23 | 22 | 23 | 15 |
| Muscovite | - | - | 2 | - | - |
| Garnet | 6.0 | 6 | 3 | 3 | 1 |

*Localization:* 7/B-85 - Benova dolina Valley; 12/B-85 - to the north of Kanné dolina Valley; 2/B-85 - Veľká Kamenná dolina Valley; 6/B-85 - Dlhá dolina Valley, altitude 700 m; 13/B-85 Kanné dolina Valley.

Amidst the gneiss-amphibolite complex migmatite bodies occur of granitic and tonalitic composition. They have blastogranitic or hipidiomorphic texture. Among felsic minerals, feldspars and quartz are most common (30 - 40 and 30 vol.%, respectively), perthitic K-feldpar is less common (10 - 15 vol.%). Femic minerals are represented by biotite (10 - 15 vol.%) and garnet (to 1 vol. %). In melanocratic, tonalitic varieties the contents of garnet and biotite, accompanied by amphibole, increases and that of orthoclase decreases. The magmatic mineral association of the first generation is partly replaced by a lower temperature mineral association represented by muscovite and microcline. In this stage, plagioclase (I) and orthoclase (I) are replaced by microcline, microcline-perthite or muscovite, and biotite and alumosilicates by muscovite.

Hydrothermal-metasomatic alterations of various degree occur in gneisses and migmatites, represented by the association of muscovite + chlorite + epidote-zoizite.

The latest retrograde alterations are related to the formation of mylonite zones cataclastic deformation and weak recrystallization of quartz, sericitization and argilitization of feldspars, breakdown of femic minerals to chlorite, epidote, calcite and Fe-Ti oxides.

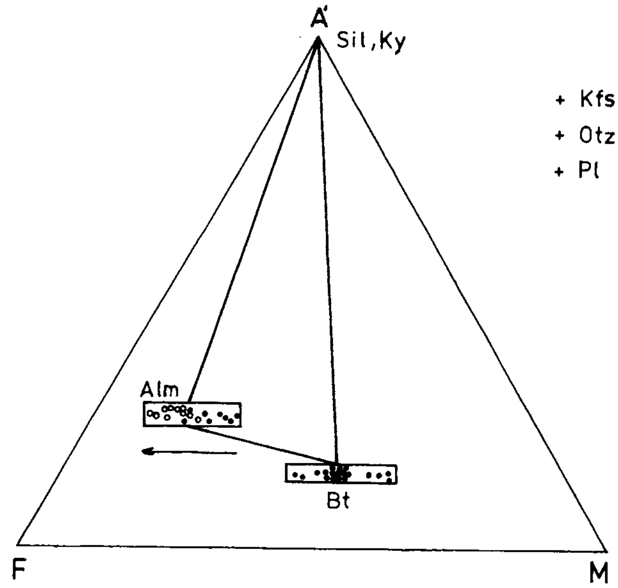


**Fig. 2.** Interpretation of phase relations based on the garnet and biotite compositions, A'FM projection after Reinhardt (1968). The arrow shows the change in chemical compositions of garnet from core (solid circles) to rim (open circles).

## Characterization of minerals

*Garnet:* Garnet porphyroblasts are damaged to a various degree by cataclastic deformations. They contain random inclusions of quartz, opaques and apatite. Chloritization occurs sporadically. Garnets are optically homogeneous without apparent zoning. They have composition of almandine with relatively high content of the pyrope component (Tab. 2). The amount of $Al^{VI}$ ranges about 2 indicating probably a low content of ferric iron in their structure. Therefore, the garnet composition may be considered solid solution with Alm-Prp-Grs-Sps end members (Fig. 3). The content of almandine end member ranges about 66 - 75 wt. %.

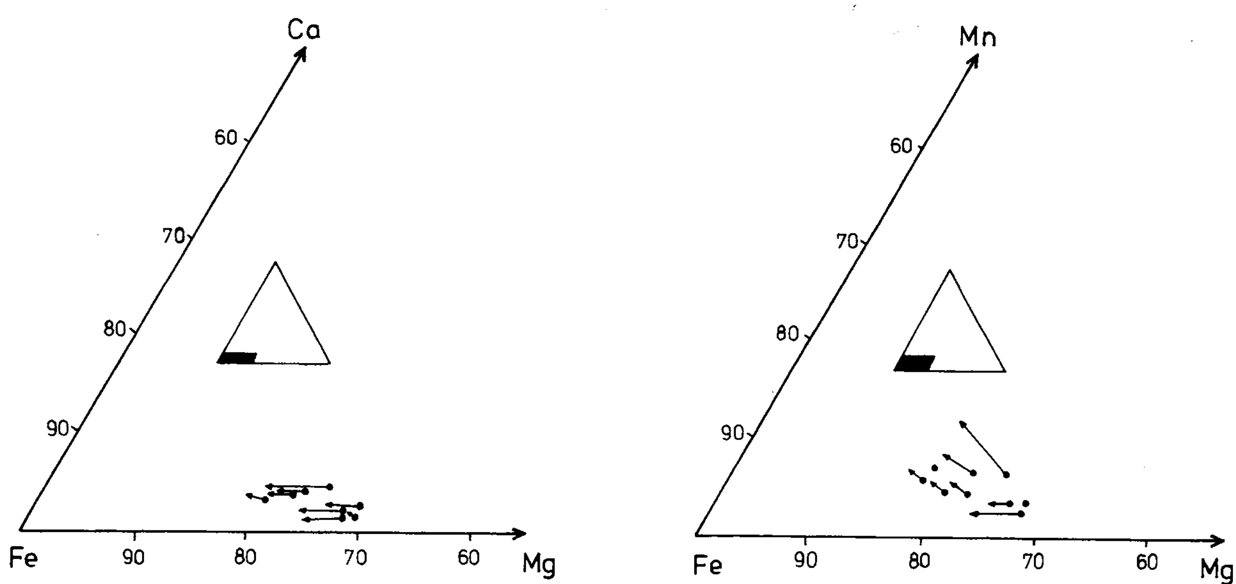


**Fig. 3.** Chemical composition of garnets in terms of Ca-Fe-Mg and Mn-Fe-Mg. The arrow shows changes in garnet compositions from core (solid circles) to rim (open circles).

**Table 2:** Garnet compositions.

| | 7/B-85 | | 12/B-85 A | | | | 12/B-85 B | | | 2/B-85 | | 6/B-85 | | 13/B-85 A | | | | | | 13/B-85B |
|---|---|---|---|---|---|---|---|---|---|---|---|---|---|---|---|---|---|---|---|---|
| | $Grt_1$(r) | $Grt_2$(c) | $Grt_1$(r) | $Grt_2$(c) | $Grt_3$(c) | $Grt_4$(r) | $Grt_1$(c) | $Grt_2$(c) | $Grt_3$(r) | $Grt_1$(r) | $Grt_2$(c) | $Grt_1$(r) | $Grt_2$(c) | $Grt_1$ | $Grt_2$ | $Grt_3$ | $Grt_4$ | $Grt_5$ | $Grt_6$ | $Grt_1$(r) |
| $SiO_2$ | 37.70 | 37.86 | 38.12 | 38.06 | 38.07 | 37.69 | 38.04 | 37.90 | 37.37 | 37.23 | 37.78 | 37.16 | 37.68 | 36.78 | 37.46 | 37.22 | 37.29 | 37.13 | 37.17 | 36.24 |
| $TiO_2$ | 0.04 | 0.00 | 0.02 | 0.03 | 0.04 | 0.06 | 0.01 | 0.01 | 0.01 | 0.00 | 0.00 | 0.00 | 0.01 | 0.02 | 0.01 | 0.00 | 0.01 | 0.02 | 0.04 | 0.00 |
| $Al_2O_3$ | 22.39 | 22.41 | 22.44 | 22. 26 | 22.39 | 22.44 | 22.43 | 22.67 | 22.04 | 21:89 | 21.48 | 22.32 | 22.21 | 22.04 | 21.78 | 22.03 | 22.20 | 21.89 | 20.53 | 21.60 |
| FeO | 32.68 | 32.33 | 30.43 | 30.33 | 31.39 | 32.26 | 31.07 | 30.85 | 31.91 | 30.44 | 30.53 | 30.39 | 30.05 | 32.87 | 33.21 | 32.69 | 32.82 | 32.10 | 33.61 | 31.03 |
| MnO | 2.03 | 1.74 | 1.13 | 1.04 | 1.31 | 1.19 | 1.09 | 1.11 | 1.04 | 3.05 | 2.50 | 4.97 | 2.45 | 2.15 | 1.85 | 2.02 | 2.13 | 2.26 | 2.56 | 2.64 |
| MgO | 5.24 | 5.77 | 7.02 | 6.90 | 6.79 | 6.20 | 6.87 | 6.95 | 5.83 | 4.42 | 5.43 | 4.50 | 6.08 | 4.60 | 5.01 | 4.81 | 4.64 | 3.92 | 4.02 | 4.35 |
| CaO | 0.93 | 0.93 | 0.81 | 0.81 | 0.88 | 0.83 | 0.81 | 0.81 | 0.81 | 1.15 | 1.20 | 1.26 | 1.38 | 1.01 | 1.04 | 1.04 | 0.92 | 0.98 | 1.03 | 0.87 |
| $Cr_2O_3$ | 0.05 | 0.02 | 0.00 | 0.00 | 0.00 | 0.00 | 0.00 | 0.00 | 0.01 | 0.00 | 0.00 | 0.03 | 0.02 | 0.04 | 0.06 | 0.05 | 0.00 | 0.06 | 0.00 | 0.01 |
| Total | 101.06 | 101.06 | 99.97 | 99.43 | 100.87 | 100.67 | 100.32 | 100.30 | 99.02 | 98.19 | 98.92 | 100.63 | 99.88 | 99.51 | 100.42 | 99.86 | 100.01 | 98.36 | 98.96 | 96.74 |
| | | | | | | | | | | | | | | | | | | | | |
| Si | 2.958 | 2.960 | 2.976 | 2.987 | 2.962 | 2.951 | 2.969 | 2.956 | 2.972 | 2.998 | 3.011 | 2.943 | 2.966 | 2.945 | 2.968 | 2.962 | 2.963 | 2.995 | 3.012 | 2.970 |
| $Al^{IV}$ | 0.042 | 0.040 | 0.024 | 0.013 | 0.038 | 0.049 | 0.031 | 0.044 | 0.028 | 0.002 | 0.000 | 0.057 | 0.034 | 0.055 | 0.032 | 0.038 | 0.037 | 0.005 | 0.000 | 0.30 |
| $Al^{VI}$ | 2.028 | 2.025 | 2.041 | 2.045 | 2.016 | 2.021 | 2.031 | 2.040 | 2.038 | 2.075 | 2.018 | 2.027 | 2.027 | 2.025 | 2.002 | 2.028 | 2.043 | 2.077 | 1.961 | 2.056 |
| Ti | 0.002 | 0.000 | 0.001 | 0.002 | 0.002 | 0.004 | 0.001 | 0.001 | 0.000 | 0.000 | 0.000 | 0.000 | 0.001 | 0.001 | 0.001 | 0.000 | 0.001 | 0.001 | 0.002 | 0.000 |
| Cr | 0.003 | 0.001 | 0.000 | 0.000 | 0.000 | 0.000 | 0.000 | 0.000 | 0.001 | 0.000 | 0.000 | 0.002 | 0.001 | 0.003 | 0.004 | 0.003 | 0.000 | 0.004 | 0.000 | 0.001 |
| $Fe^{+2}$ | 2.144 | 2.114 | 1.987 | 1.990 | 2.043 | 2.112 | 2.028 | 2.012 | 2.123 | 2.050 | 2.035 | 2.013 | 1.978 | 2.201 | 2.201 | 2.175 | 2.181 | 2.166 | 2.278 | 2.117 |
| Mn | 0.135 | 0.115 | 0.075 | 0.069 | o.086 | 0.079 | 0.072 | 0.073 | 0.070 | 0.208 | 0.169 | 0.333 | 0.163 | 0.146 | 0.124 | 0.136 | 0.143 | 0.154 | 0.176 | 0.183 |
| Mg | 0.613 | 0.673 | 0.817 | 0.807 | 0.788 | 0.724 | 0.799 | 0.808 | 0.691 | 0.531 | 0.645 | 0.531 | 0.714 | 0.549 | 0.592 | 0.571 | 0.550 | 0.471 | 0.486 | 0.531 |
| Ca | 0.078 | 0.078 | 0.068 | 0.068 | 0.073 | 0.070 | 0.068 | 0.068 | 0.069 | 0.099 | 0.102 | 0.107 | 0.116 | 0.087 | 0.088 | 0.089 | 0.078 | 0.085 | 0.089 | 0.076 |
| Alm | 72.12 | 70.92 | 67.43 | 67.82 | 68.32 | 70.78 | 68.35 | 67.95 | 71.87 | 70.99 | 68.95 | 67.40 | 65.55 | 73.73 | 73.14 | 73.15 | 73.87 | 75.20 | 75.21 | 72.87 |
| Andr | 0.12 | - | 0.06 | 0.09 | 0.12 | 0.18 | 0.03 | 0.03 | 0.03 | - | - | - | 0.03 | 0.06 | 0.03 | - | 0.03 | 0.06 | 0.12 | - |
| Grs | 2.51 | 2.61 | 2.24 | 2.23 | 2.34 | 2.15 | 2.25 | 2.26 | 2.31 | 3.43 | 3.47 | 3.58 | 3.88 | 2.84 | 2.90 | 2.98 | 2.62 | 2.88 | 2.83 | 2.62 |
| Pyr | 20.61 | 22.56 | 27.73 | 27.50 | 26.34 | 24.25 | 26.94 | 27.29 | 23.41 | 18.37 | 21.86 | 17.79 | 24.00 | 18.39 | 19.67 | 19.19 | 18.62 | 16.37 | 16.04 | 18.21 |
| Spess | 4.54 | 3.87 | 2.54 | 2.36 | 2.89 | 2.64 | 2.43 | 2.48 | 2.37 | 7.20 | 5.72 | 11.16 | 5.50 | 4.88 | 4.13 | 4.58 | 4.86 | 5.36 | 5.80 | 6.28 |
| Uvar | 0.10 | 0.04 | - | - | - | - | - | - | 0.02 | - | - | 0.06 | 0.04 | 0.08 | 0.12 | 0.11 | - | 0.13 | - | 0.02 |

The high contents of pyrope end member (18 - 27 wt. %) indicate high grade metamorphic conditions. Such a high magnesium content in garnets is generally reported for garnets of granulite facies metapelites. In the Western Carpathians were reported similar relictic garnets with increased contents of pyrope end member in gneisses of the Suchý, Malá Magura, Malá Fatra (Korikovsky et al. 1987; Hovorka et al. 1987; Méres & Hovorka 1989) and Branisko (Vozárová & Krištín 1986) crystalline complexes. In all the mentioned cases the garnets show relatively significant regressive zoning.

In the garnets of the northern Branisko Mts. only slight changes in Fe, Mg, Mn concentrations are seen from core to rim. The cores are almost homogenised, only at rims Mg decreases and Fe, Mn increase. The diffusion profile of garnet is flat (Fig. 4) reflecting exchange reactions only at grain rims. No, or only insignificant, changes were observed in Ca distribution. In the direction from core to rim, the grossular content either does not change or slightly increases close to the edge of grain due to the lower Ca diffusivity. The zoning of Fe, Mg, Mn at grain rims is significant which probably reflect resorption of garnet and exchange reactions during cooling.

*Biotite:* Chemical composition of biotite (Tab. 3) does not show any significant changes. In the basic classification diagram (Fig. 5) plot two slightly differing biotite groups.

Biotites from the sample 12/B-85 have relatively higher Mg contents ($N^{Bi}_{Mg}$ = 0.57 - 0.59) and somewhat lower $Al^{VI}$ value. Biotites from other samples have $N^{Bi}_{Mg}$ = 0.49 - 0.52 with correspondingly higher $Al^{VI}$ (0.80 - 0.87). After the data of Guidotti (in Bailey et al. 1984) in the biotites from high -grade Al-saturated metamorphites (Sil + Kfs without Mus) the $Al^{VI}$ content ranges between 0.7 - 1.0. By contrast, a slight decrease of $Al^{VI}$ occurs in biotites from the Sil + Kfs association under further increasing P and T.

The $Ti^{VI}$ contents are higher than those reported for the lower temperature amphibolite facies (< 0.25) in all biotite samples. The highest $Ti^{VI}$ contents are again in 12/B-85 biotite ($Ti^{VI}$= 0.35 - 0.43). Ti vs Mg contents relations are vague, only in 12/B-85 biotite with the increasing $Ti^{VI}$ also $N^{Bi}_{Mg}$ slightly increases (Tab. 3). To the contrary, with increasing Mg the tetrahedral Al/Si ratio decreases.

*Plagioclases:* The An contents range between 25 - 31 mol% (corresponding to Ca-oligoclase and Na-andesine, Tab. 4) in all analysed rock types. The Or content ranges about 1 %, in one case attains 3 %. The Ti, Mg and Mn contents are negligible, the FeO varies about 0.1 %. Majority of plagioclase grains do not show a zoning. The present grains with sericitised cores possibly reflect composition differences due to oscillatory growth of grains. Twins according to albite, pericline and Karlsbad laws are common. Rarely, the plagioclases are antiperthitic.

*Orthoclase:* It forms xenomorphic, slightly elongated, oval and often perthitic grains. The perthitic K-feldspar is represented by mesoperthite.

*Sillimanite/kyanite:* From these $Al_2SiO_5$ polymorphs sillimanite is more frequent. It forms well developed long prismatic crystals, in texture significantly preferentially oriented and associated with biotite, quartz, K-feldspar and plagioclase. The crystals of kyanite, if present, occur in texture individually, being partly replaced by sillimanite. In few cases desintegrated kyanite grains were found in a sillimanite aggregate. Based on this observations, we suppose that sillimanite has formed by metamorphic reactions instead of garnet and K-feldspar, and also instead of original kyanite.

*Accessory minerals:* Magnetite and ilmenite are present among opaque minerals. They form either inclusions in garnet or occur as individual grains outside of garnet. Minute rutile grains are associated with ilmenite. The association of accessories is poor, besides rutile only zircons were found.

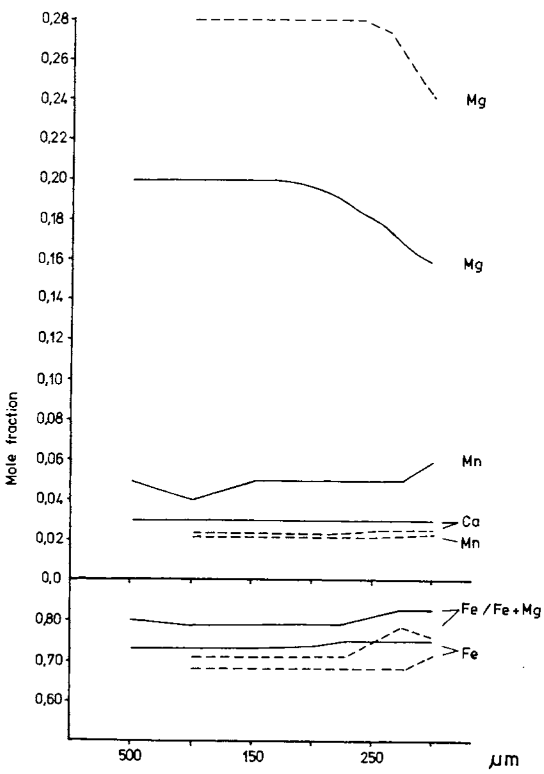


**Fig. 4.** Garnet zoning expressed in the relationship of Mg, Fe, Mn, Ca molar fractions, and Fe/(Fe+Mg) ratio *vs.* grain radius. Solid line - sample 13/B-85; dashed line - sample 12/B-85.

## P-T conditions of metamorphism

The calibrations of garnet-biotite geothermometer after Ferry & Spear (1978), Perchuk et al. (1983), Ganguly & Saxena (1984) and Indares & Martignole (1985) were used for temperature determinations. The garnet - plagioclase - sillimanite - quartz geobarometer was used for metamorphic pressure estimates in the calibrations of Newton & Haselton (1981), Koziol & Newton (1988) and Powell & Holland (1988). The results of calculations vary both in temperature and pressure values (Tab. 5).

The results of geothermometry based on Ferry & Spear's (1978) and Hodges & Spear's (1982) calibrations on the one hand, and those of Indares & Martignole (1985) and Ganguly & Saxena (1984) on the other hand, differ significantly almost in all samples. The differences in calculations range within 70 - 150 °C. The results after Perchuk et al. (1983) vary also being generally lower than those after Ferry & Spear (1978) and approaching rather the second group of authors.

The results of thermodynamic parameters calculations in natural associations of coexisting Mg-Fe silicates are influenced by relation of distribution coefficient ($K_D$) to fractionation of oxygen isotopes betwen quartz and magnetite (Goldman & Albee 1977), to Ca, Mn contents in garnet and to $Fe^{3+}$, Ti, $Al^{3+}$ contents in biotite (Indares & Martignole 1985). The $X_{Ca}$

**Table 3:** Biotite compositions.

| | 7/B-85 | | | 12/B-85 A | | 12/B-85 B | | 2/B-85 | | 6/B-85 | | | | | 13/B-85 A | | | | 13/B-85 B | |
|---|---|---|---|---|---|---|---|---|---|---|---|---|---|---|---|---|---|---|---|---|
| | $Bt_1$ | $Bt_2$ | $Bt_3$ | $Bt_1$ | $Bt_2$ | $Bt_1$ | $Bt_2$ | $Bt_1$ | $Bt_2$ | $Bt_1$ | $Bt_2$ | $Bt_3$ | $Bt_4$ | $Bt_5$ | $Bt_1$ | $Bt_2$ | $Bt_3$ | $Bt_4$ | $Bt_1$ | $Bt_2$ |
| $SiO_2$ | 35.68 | 35.45 | 34.84 | 35.48 | 36.46 | 35.78 | 36.29 | 35.20 | 35.25 | 35.00 | 34.16 | 35.41 | 34.44 | 35.17 | 35.67 | 35.17 | 35.55 | 34.19 | 34.60 | 35.68 |
| $TiO_2$ | 3.11 | 3.03 | 3.28 | 3.12 | 3.64 | 3.82 | 3.63 | 2.15 | 2.72 | 2.84 | 3.08 | 2.76 | 2.86 | 2.34 | 3.43 | 3.25 | 2.50 | 2.67 | 3.03 | 3.30 |
| $Al_2O_3$ | 18.92 | 19.17 | 18.88 | 18.95 | 19.16 | 18.86 | 19.34 | 19.06 | 18.23 | 19.24 | 19.02 | 19.41 | 19.07 | 18.82 | 19.47 | 19.51 | 19.25 | 19.79 | 19.06 | 19.24 |
| FeO | 18.65 | 16.65 | 18.15 | 15.43 | 14.85 | 15.17 | 14.52 | 17.73 | 17.68 | 17.27 | 19.48 | 17.74 | 19.57 | 18.11 | 17.63 | 17.38 | 18.11 | 17.87 | 17.26 | 16.49 |
| MnO | 0.20 | 0.15 | 0.09 | 0.00 | 0.06 | 0.00 | 0.00 | 0.14 | 0.14 | 0.17 | 0.28 | 0.27 | 0.24 | 0.32 | 0.14 | 0.12 | 0.21 | 0.18 | 0.09 | 0.06 |
| MgO | 9.18 | 9.94 | 9.97 | 11.32 | 11.77 | 11.37 | 11.86 | 9.96 | 9.76 | 9.31 | 7.86 | 9.76 | 8.35 | 10.33 | 9.61 | 9.70 | 9.91 | 9.79 | 10.05 | 9.53 |
| CaO | 0.00 | 0.01 | 0.00 | 0.00 | 0.00 | 0.02 | 0.00 | 0.00 | 0.00 | 0.00 | 0.00 | 0.00 | 0.00 | 0.00 | 0.02 | 0.00 | 0.00 | 0.00 | 0.02 | 0.01 |
| $Na_2O$ | 0.12 | 0.15 | 0.16 | 0.21 | 0.22 | 0.26 | 0.25 | 0.13 | 0.17 | 0.27 | 0.14 | 0.20 | 0.06 | 0.02 | 0.14 | 0.22 | 0.36 | 0.29 | 0.06 | 0.19 |
| $K_2O$ | 8.95 | 8.57 | 8.43 | 8.99 | 8.56 | 9.64 | 9.10 | 9.25 | 8.80 | 9.86 | 9.92 | 9.28 | 10.03 | 9.21 | 9.76 | 9.78 | 9.34 | 9.27 | 9.63 | 8.74 |
| $Cr_2O_3$ | 0.00 | 0.06 | 0.02 | 0.02 | 0.03 | 0.00 | 0.13 | 0.00 | 0.04 | 0.03 | 0.07 | 0.03 | 0.00 | 0.05 | 0.00 | 0.03 | 0.02 | 0.04 | 0.05 | 0.03 |
| Total | 94.81 | 93.18 | 93.82 | 93.52 | 94.75 | 94.92 | 95.12 | 93.62 | 92.79 | 93.81 | 94.01 | 94.86 | 94.62 | 94.37 | 95.87 | 95.16 | 95.25 | 94.09 | 93.85 | 93.27 |

| | | | | | | | | | | | | | | | | | | | | |
|---|---|---|---|---|---|---|---|---|---|---|---|---|---|---|---|---|---|---|---|---|
| Si | 5.42 | 5.42 | 5.34 | 5.39 | 5.42 | 5.37 | 5.39 | 5.41 | 5.46 | 5.38 | 5.32 | 5.37 | 5.32 | 5.38 | 5.36 | 5.33 | 5.38 | 5.25 | 5.32 | 5.44 |
| $Al^{IV}$ | 2.58 | 2.58 | 2.66 | 2.61 | 2.58 | 2.63 | 2.61 | 2.59 | 2.54 | 2.62 | 2.68 | 2.63 | 2.68 | 2.62 | 2.64 | 2.67 | 2.62 | 2.75 | 2.68 | 2.56 |
| $Al^{VI}$ | 0.81 | 0.87 | 0.74 | 0.78 | 0.78 | 0.70 | 0.77 | 0.86 | 0.78 | 0.86 | 0.80 | 0.84 | 0.80 | 0.77 | 0.80 | 0.81 | 0.82 | 0.83 | 0.76 | 0.90 |
| Ti | 0.36 | 0.35 | 0.38 | 0.36 | 0.41 | 0.43 | 0.41 | 0.25 | 0.32 | 0.33 | 0.36 | 0.32 | 0.33 | 0.27 | 0.39 | 0.37 | 0.28 | 0.31 | 0.35 | 0.38 |
| Cr | 0.00 | 0.01 | 0.00 | 0.00 | 0.00 | 0.00 | 0.00 | 0.00 | 0.00 | 0.00 | 0.01 | 0.00 | 0.00 | 0.01 | 0.00 | 0.00 | 0.00 | 0.01 | 0.01 | 0.00 |
| $Fe^{+2}$ | 2.37 | 2.13 | 2.33 | 1.96 | 1.85 | 1.90 | 1.80 | 2.28 | 2.29 | 2.22 | 2.54 | 2.25 | 2.53 | 2.32 | 2.21 | 2.20 | 2.29 | 2.29 | 2.22 | 2.11 |
| Mn | 0.03 | 0.02 | 0.01 | 0.00 | 0.01 | 0.00 | 0.00 | 0.02 | 0.02 | 0.02 | 0.04 | 0.04 | 0.03 | 0.04 | 0.02 | 0.02 | 0.03 | 0.02 | 0.01 | 0.01 |
| Mg | 2.08 | 2.27 | 2.28 | 2.56 | 2.61 | 2.54 | 2.62 | 2.28 | 2.25 | 2.13 | 1.82 | 2.21 | 1.92 | 2.35 | 2.15 | 2.19 | 2.24 | 2.24 | 2.30 | 2.17 |
| Ca | 0.00 | 0.00 | 0.00 | 0.00 | 0.00 | 0.00 | 0.00 | 0.00 | 0.00 | 0.00 | 0.00 | 0.00 | 0.00 | 0.00 | 0.00 | 0.00 | 0.00 | 0.00 | 0.00 | 0.00 |
| Na | 0.04 | 0.05 | 0.05 | 0.06 | 0.06 | 0.08 | 0.07 | 0.04 | 0.05 | 0.08 | 0.04 | 0.06 | 0.02 | 0.01 | 0.04 | 0.07 | 0.11 | 0.09 | 0.02 | 0.06 |
| K | 1.74 | 1.67 | 1.65 | 1.74 | 1.62 | 1.85 | 1.72 | 1.81 | 1.74 | 1.90 | 1.97 | 1.80 | 1.98 | 1.80 | 1.87 | 1.89 | 1.80 | 1.82 | 1.89 | 1.70 |

and $X_{Mn}$ values in garnets of the northern part of Branisko Mts. are low and they should not, therefore, influence the calculated temperature in majority of samples. Ganguly & Saxena (1984) suggested a calculation of the non-ideality of garnets in temperature interval 500-700° C. However, these parameters are not applicable for garnets with the Alm/Prp ratio <3. All analysed garnets have this ratio lower than 3, except 13/B and 7/B with slightly higher values. Indares & Martignole (1985) studied the non-ideality of garnet in low Ca-Mn solid solutions and found that in granulite facies garnets the Ferry and Spear's calibration gives higher values in the range +40 °C.

In biotites the substitution of $Fe^{3+}$, Ti and $Al^{VI}$ for $Fe^{2+}$ and Mg is important. A simple petrological check of the $Fe^{3+}$ amount in metapelites is the coexistence of biotite with magnetite and/or hematite indicating oxidation conditions (Guidotti et al. 1977). In biotites from Al-, Si- and Ti-saturated metapelites and coexisting with magnetite the authors determined up to 10 - 13 % of $^{VI}Fe^{3+}$ (of total Fe) contrasting with only 4 % of $^{VI}Fe^{3+}$ in biotites coexisting with graphite. Moreover, they found that the amount of $Fe^{3+}$ is independent of metamorphic degree and association of silicate minerals.

In the analysed rocks magnetite is absent or scarce (7/B-85) and, therefore, we do not suppose any significant $Fe^{3+}$ involvement in the substitution of $Al^{VI}$ and Ti for $R^{2+}$.

The distribution of $Al^{VI}$ and Ti relative to Mg/Fe values is variable in analysed biotites (Fig. 6). A relatively more distinct, positive relation seems to exist only in sample 12/B-85. Other samples of the analysed file do not show any significant dependence of $Al^{VI}$ and Ti on the increasing $Mg/Fe^{2+}$. Based on this, we suppose no significant influence of the exchange $Al^{VI}$ and Ti for $R^{2+}$ on the $Mg/Fe^{2+}$ values in biotites and, therefore, on the calculated temperatures. A computer model of cooling of granulite facies rocks with the mineral association Grt + Bt + Sil + Kfs + Pl + Qtz was presented by Spear & Florence (1992). The results of this modelling showed that any petrological interpretation of P-T trends of this rock group has to take into account (1) types of retrograde reactions occurring during cooling of sample, (2) the modal abundance of biotite and plagioclase in equilibrium with garnet in given time interval, (3) the size of analysed garnet and (4) the cooling rate.

The basic problem of interpretation of thermobarometric calculations is that there are no priority criteria for determining of equilibrium compositions of mineral phases during peak of metamorphism. Spear & Florence (1992) showed by their modelling how important is to determine whether, upon cooling, only exchange reactions plus diffusion (Fe - Mg and Mn - Fe in garnet and biotite), or net transfer reactions (Grt + Kfs + $H_2O$ = Sil + Bt + Qtz; An = Grs + Sil + Qtz) occur in sample. It should be stressed that in all analysed samples from the northern Branisko gneiss-amphibolite complex the evidence is found of the common occurrence of both exchange and net transfer reactions. The structural evidence is seen in the low modal content of garnet compared with biotite ($V_g/V_b$ = 0.26 - 0.07) and in the irregular shape of garnets often with lobate forms (Pl. 1: 1, 2, 3) indicating their resorption. Another significant evidence of the garnet resorption is the existence of a relatively homogeneous core with a more distinct zoning occurring only at grain rims.

Since the volume proportion of garnet compared to biotite is low in the analysed samples, we suppose a more significant decrease of garnet due to the reactions through which garnet and K-feldspar gave rise to biotite, sillimanite and quartz. This change reflects the retrograde processes during cooling and decompression which are controlled by the access of $H_2O$ into the whole system.

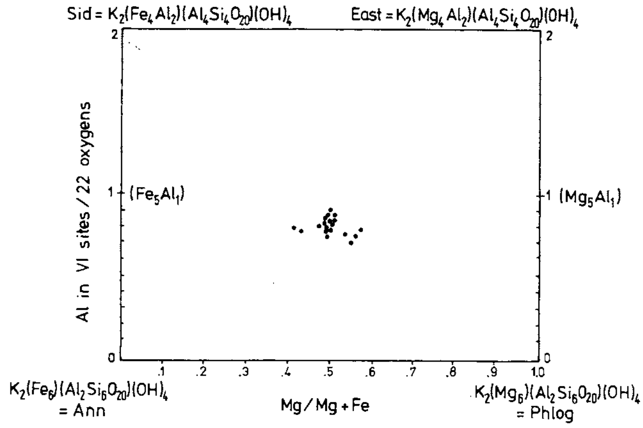


**Fig. 5.** Biotite compositions in terms of $Al^{VI}$ *vs.* Mg/(Mg+Fe).

Phase relations in the mineral assemblage Grt + Bt + Kfs + Pl + Sil + Qtz + $H_2O$ are controlled, besides the above mentioned exchange and metamorphic reactions, also by the reactions supporting equilibrium relations Ca in garnet and in plagioclase. Therefore, if garnet resorption and decrease occurs in sample the increase of plagioclase has also to occur. The finding of zoning in garnet and distribution of An-component in plagioclase is a presumption of the realistic P-T estimate.

The zoning profile of Fe/Fe + Mg, Fe and Mn in garnets of the Branisko gneiss-amphibolite complex is flat in grain centres and rises at rims. The Mg profile is also flat in centres but at rims drops down. A different zoning was observed in the case of Ca. The zoning profile is flat almost across the whole grain or shows a very slight rise at rims (Tab. 2, Fig. 4). From the comparison with model determinations of P-T trends of granulites in the system CaO + $Na_2O$ + Mn FMKASH (Spear & Florence 1992) it can be supposed that only a relatively small amount of plagioclase reacted with garnet rims in these garnets and, hence, a major part of plagioclase should be in equilibrium with garnet cores.

The thermobarometric parameters for the Branisko gneiss-amphibolite complex were calculated from cores of garnet and biotite which is in analysed samples considerably homogenised. It is confirmed by microprobe analyses of biotite (Tab. 3) which show that there are no significant differences within one sample (i.e. at biotite-garnet contacts or within matrix of the rock). This follows from the nature of exchange reactions between garnet and biotite in high-grade metamorphites when the diffusion exchange of Fe-Mg in biotite continues even when the net transfer reactions had ceased and garnet cores had been stabilised. Biotite in the whole sample got into equilibrium with garnet rims (matrix biotite after Spear & Florence 1992).

The temperatures calculated from garnet cores and matrix biotites in the Branisko gneiss-amphibolite complex range between 769 - 673 °C with the exception of sample 6/B-85 which gives a considerably higher temperature of 857 °C, calculated from garnet core. With respect to the identified retrograde reaction types, the homogenisation of matrix biotite and its significant modal content compared to that of garnet as well as the relatively small size of garnet grains (< 0.5 mm) such a scatter of values is to be expected. Model temperatures calculated from the cores of garnet range between 700 - 750° C (Spear & Florence 1992).

**Table 4:** Plagioclase compositions.

| | 7/B-85 | | | | 12/B-85A | 12/B-85B | 2/B-85 | | 6/B-85 | 13/B-85A | 13/B-85B | |
|---|---|---|---|---|---|---|---|---|---|---|---|---|
| $SiO_2$ | 59.30 | 59.13 | 59.13 | 59.13 | 61.32 | 60.96 | 59.50 | 61.24 | 61.10 | 61.89 | 60.44 | 59.87 |
| $TiO_2$ | 0.02 | 0.00 | 0.00 | 0.00 | 0.02 | 0.00 | 0.00 | 0.02 | 0.00 | 0.00 | 0.04 | 0.03 |
| $Al_2O_3$ | 25.01 | 24.87 | 24.88 | 24.87 | 24.93 | 24.39 | 24.82 | 24.70 | 24.33 | 24.44 | 24.16 | 25.64 |
| FeO | 0.12 | 0.03 | 0.03 | 0.03 | 0.05 | 0.14 | 0.05 | 0.08 | 0.00 | 0.05 | 0.03 | 0.09 |
| MnO | 0.09 | 0.04 | 0.04 | 0.04 | 0.02 | 0.00 | 0.00 | 0.01 | 0.00 | 0.05 | 0.00 | 0.00 |
| MgO | 0.00 | 0.00 | 0.00 | 0.00 | 0.00 | 0.00 | 0.00 | 0.02 | 0.00 | 0.00 | 0.02 | 0.01 |
| CaO | 6.20 | 6.35 | 6.42 | 6.42 | 4.94 | 5.37 | 6.05 | 5.74 | 5.61 | 5.35 | 5.15 | 6.62 |
| $Na_2O$ | 7.90 | 7.80 | 7.88 | 7.80 | 8.33 | 8.47 | 8.14 | 8.36 | 8.14 | 8.66 | 8.60 | 7.89 |
| $K_2O$ | 0.10 | 0.09 | 0.09 | 0.09 | 0.32 | 0.45 | 0.09 | 0.08 | 0.15 | 0.11 | 0.21 | 0.13 |
| $Cr_2O_3$ | 0.00 | 0.00 | 0.00 | 0.00 | 0.06 | 0.00 | 0.04 | 0.00 | 0.00 | 0.01 | 0.03 | 0.01 |
| Total | 98.74 | 98.31 | 98.47 | 98.38 | 99.99 | 99.78 | 98.69 | 100.25 | 99.33 | 100.56 | 98.68 | 100.29 |

| | | | | | | | | | | | | |
|---|---|---|---|---|---|---|---|---|---|---|---|---|
| Si | 2.67 | 2.68 | 2.67 | 2.68 | 2.72 | 2.72 | 2.68 | 2.71 | 2.73 | 2.73 | 2.72 | 2.66 |
| Al | 1.33 | 1.33 | 1.33 | 1.33 | 1.30 | 1.28 | 1.32 | 1.29 | 1.28 | 1.27 | 1.28 | 1.34 |
| Ca | 0.30 | 0.31 | 0.31 | 0.31 | 0.24 | 0.26 | 0.29 | 0.27 | 0.27 | 0.25 | 0.25 | 0.32 |
| Na | 0.69 | 0.68 | 0.69 | 0.68 | 0.72 | 0.73 | 0.71 | 0.72 | 0.70 | 0.74 | 0.75 | 0.68 |
| K | 0.01 | 0.01 | 0.01 | 0.01 | 0.02 | 0.03 | 0.01 | 0.00 | 0.01 | 0.01 | 0.01 | 0.01 |
| Alb | 69.0 | 68.0 | 68.3 | 68.0 | 73.9 | 71.6 | 70.5 | 72.7 | 71.4 | 74.0 | 74.2 | 67.8 |
| An | 30.0 | 31.0 | 30.7 | 31.0 | 24.2 | 25.5 | 30.0 | 27.3 | 27.6 | 25.0 | 24.6 | 31.4 |
| Ort | 1.0 | 1.0 | 1.0 | 1.0 | 1.9 | 2.9 | 0.5 | - | 1.0 | 1.0 | 1.2 | 0.8 |

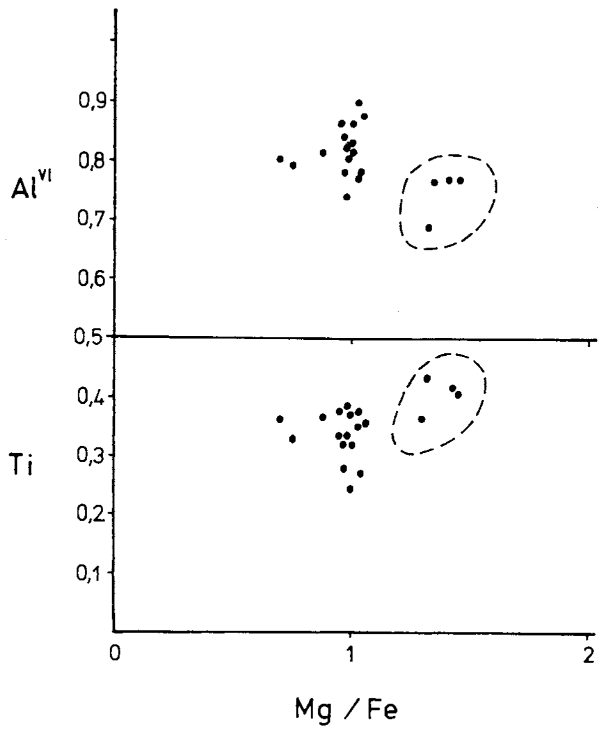


**Fig. 6.** Biotite Mg/Fe ratio *vs.* $Al^{VI}$ and Ti. The dashed line field corresponds to the biotites of 12/B-85 sample.

Closest to these model values are the temperatures calculated from garnet cores from the samples 7/B-85, 12/B-85 and 2/B-85 (Tab. 5). Relatively lower core-based temperatures were obtained from the sample 13/B-85 which was caused by retrograde reactions producing sillimanite and being accompanied by a marked resorption of garnet (Pl. 1: 6; Pl. 2: 6, 8). In minute garnet grains the composition changes occurred not only at rims but also in centres of garnet and the calculated temperatures, therefore, do not reflect peak metamorphism conditions because garnet cores reequilibrated with matrix biotite.

An opposite case was found in sample 6/B-85 which yielded a high core temperature (857 °C). In this sample garnets have the size of 1 - 2 mm with a significant increase of Mn at rims (5.50 - 11.60). It would suggest that a considerable part of garnet rims was consumed in exchange reactions. The exchange reactions in garnet core ended much earlier than the matrix biotite became stabilized. Thus, the garnet core composition remained unchanged, meanwhile the matrix biotite having significantly higher Fe/Mg than at the culmination of metamorphism. This is a probable cause of the high temperatures calculated from the garnet core in this sample.

In spite of all the mentioned facts the regression trend appeared in the temperatures calculated form garnet rim and matrix biotite. Garnet rim-matrix biotite temperatures range between 590 - 682 °C being in individual grains by 60 to 100 °C (in average) lower than in cores. The pressures calculated by Grt-Bt-Pl-Sil barometer from garnet cores range between 390 - 630 MPa, in sample 6/B-85 up to 870 MPa. The values calculated from garnet rims are lower, 260 - 420 MPa, however, having the same scatter as those from garnet cores (Tab. 5). This scatter of values suggests that not all plagioclases reacted with garnet during the change of metamorphic conditions. It is not simple to distinguish the both plagioclase groups in microscope, this being a reason for the variability of the calculated values.

Based on the calculated thermobarometric data it can be supposed that the maximum temperatures during peak metamorphic conditions in the northern Branisko metamorphic complex were in the range 700 - 750 °C even though the garnet cores and matrix biotite do not always show the Fe/Mg ratio values corresponding to that temperature. The specific conditions, including the small garnet size and the high modal proportion of biotite compared to garnet, caused that exchange reactions in garnet cores were compensated by matrix biotite changes with the result that the calculated temperatures have approached the values corresponding the culmination of metamorphism. This reasoning is supported by the mineral composition of the rocks, mainly by the coexistence of sillimanite and K-feldspar (Pl. 1: 3, 7, 8; Pl. 2: 1, 6) in the presence of quartz and almandine with a high content of pyrope component. Based on the relics of kyanite (Pl. 1: 5, 6, 7, 8; Pl. 2: 1, 2, 4, 5) intermediate to high pressures can be supposed during the peak of metamorphism. The calculated core pressures about 400 - 600 MPa correspond to the regression stage of a metamorphic event when a stabilisation of the whole mineral assemblage occured. This proces might have reflected an isothermal uplift followed by an isobaric cooling of the whole complex. It is evidenced by the beginning of proces of sillimanite and K-feldspar replacing by the association muscovite + quartz. This would suggest that the final stage of the whole complex stabilisation was completed at temperatures above 550 °C and pressures about 300 - 400 MPa.

## Evolution of the metamorphism

Temperatures and pressures calculated by the Grt-Bt thermometer and Grt-Bt-Pl-Sill barometer yield a regressive trend in accord with the change of chemical compositions in garnet cores and rims. The high temperatures combined with medium to high pressures, evidenced by the garnet core compositions and kyanite relics, correspond probably to a relict metamorphic event (M0) having attained the P-T conditions at the boundary of granulite facies. The following uplift of the whole complex to upper parts of the Earth' crust and decompression have caused a retrograde metamorphism in P-T conditions of the higher temperature amphibolite facies (M1) which are recorded in the change of chemical composition at the contacts of garnet and biotite. The calculated regressive P-T trend is evidenced by the reducing of garnet content accompanied by sillimanite, biotite and quartz growth and the kyanite replacement by sillimanite. Related to this stage was the partial anatexis and migmatitization of the whole complex connected with $H_2O$ influx and the anatectic melt formation, separation and migration. The final stabilisation of the whole complex was determined by the reaction Sil + Kfs = Mus + Qtz corresponding to temperatures above 550 °C.

The whole complex underwent the cataclastic deformation (M2) in P-T conditions of the low-temperature greenschist facies still in pre-Permian times (evidenced in Permian conglomerates). It is characterized by the mineral assemblage muscovite-chlorite-quartz. The youngest regressive phase (M3) has a character of Alpidic dislocation metamorphism and is related to the mylonite zones formation and accompanied by clay minerals, or sericite and quartz.

The critical association Bt + Alm + Sill, with the biotite of intermediate Fe-Mg composition ($X^{Bi}_{Mg}$ = 0.5 - 0.6) and the garnet the of pyrope-almandine join ($X^{Gt}_{Fe}$ about 0.7; $X^{Gt}_{Mg}$ = 0.2 - 0.27) with only low contents of grossular and spessartine components, is stable in high temperature and pressure conditions.

**Table 5:** Thermobarometric parameters of high-grade metamorphism in crystalline rocks of the northern part of Branisko Mts.

| | 7/B-85 | | 12/B-85A | | 12/B-85B | | 2/B-85 | | 6/B-85 | | 13/B-85B | | 13/B-85A | | |
|---|---|---|---|---|---|---|---|---|---|---|---|---|---|---|---|
| | $Bt_1$ | $Bt_2$ | $Bt_2$ | $Bt_1$ | $Bt_2$ | $Bt_1$ | $Bt_1$ | $Bt_1$ | $Bt_3$ | $Bt_2$ | $Bt_1$ | Bt2 | $Bt_2$ | $Bt_2$ | $Bt_1$ |
| $Al^{VI}$ | 0.143 | 0.155 | 0.138 | 0.138 | 0.137 | 0.125 | 0.152 | 0.152 | 0.149 | 0.145 | 0.135 | 0.163 | 0.144 | 0.144 | 0.144 |
| Ti | 0.064 | 0.062 | 0.072 | 0.063 | 0.072 | 0.077 | 0.044 | 0.044 | 0.056 | 0.065 | 0.062 | 0.068 | 0.066 | 0.066 | 0.070 |
| Fe | 0.420 | 0.378 | 0.327 | 0.346 | 0.322 | 0.341 | 0.341 | 0.401 | 0.399 | 0.401 | 0.393 | 0.378 | 0.394 | 0.394 | 0.397 |
| Mn | 0.005 | 0.003 | 0.001 | 0.000 | 0.000 | 0.000 | 0.003 | 0.003 | 0.006 | 0.004 | 0.002 | 0.001 | 0.003 | 0.003 | 0.003 |
| Mg | 0.368 | 0.402 | 0.462 | 0.453 | 0.468 | 0.456 | 0.401 | 0.401 | 0.391 | 0.385 | 0.407 | 0.389 | 0.392 | 0.392 | 0.386 |
| | $Grt_1$(r) | $Grt_2$(c) | $Grt_4$(c) | $Grt_2$(c) | $Grt_3$(r) | $Grt_1$(c) | $Grt_1$(r) | $Grt_2$(c) | $Grt_1$(r) | $Grt_2$(c) | $Grt_1$(r) | $Grt_1$(r) | $Grt_3$(c) | $Grt_2$(c) | $Grt_5$(r) |
| Fe | 0.722 | 0.709 | 0.708 | 0.678 | 0.719 | 0.683 | 0.710 | 0.690 | 0.675 | 0.666 | 0.729 | 0.729 | 0.732 | 0.732 | 0.753 |
| Mn | 0.045 | 0.039 | 0.026 | 0.024 | 0.024 | 0.024 | 0.072 | 0.057 | 0.112 | 0.055 | 0.063 | 0.063 | 0.046 | 0.041 | 0.053 |
| Mg | 0.206 | 2.226 | 0.243 | 0.275 | 0.234 | 0.269 | 0.184 | 0.219 | 0.178 | 0.240 | 0.182 | 0.182 | 0.192 | 0.197 | 0.164 |
| Ca | 0.026 | 0.026 | 0.023 | 0.023 | 0.023 | 0.023 | 0.034 | 0.035 | 0.036 | 0.039 | 0.026 | 0.026 | 0.030 | 0.029 | 0.029 |
| | Pl | Pl | Pl | Pl | Pl | Pl | Pl | Pl | Pl | Pl | Pl | Pl | Pl | Pl | Pl |
| Ca | 0.307 | 0.307 | 0.243 | 0.243 | 0.255 | 0.255 | 0.289 | 0.289 | 0.276 | 0.276 | 0.245 | 0.245 | 0.250 | 0.250 | 0.250 |
| Na | 0.683 | 0.683 | 0.739 | 0.739 | 0.716 | 0.716 | 0.706 | 0.706 | 0.714 | 0.714 | 0.743 | 0.743 | 0.740 | 0.740 | 0.740 |
| Ln(K)Gt-Bi | -1.1215 | -1.2065 | -1.4162 | -1.1708 | -1.4979 | -1.2219 | -1.3517 | -1.1499 | -1.3129 | -0.9780 | -1.4245 | -1.4167 | -1.3319 | -1.3077 | -1.4969 |
| T (°C) | 757.7 | 713.3 | 621.5 | 726.5 | 590.3 | 694.5 | 682.4 | 769.1 | 704.4 | 857.1 | 641.4 | 639.9 | 673.3 | 681.3 | 611.3 |
| P (MPa) | 450 | 390 | 340 | 490 | 260 | 420 | 480 | 630 | 560 | 870 | 420 | 380 | 490 | 490 | 370 |

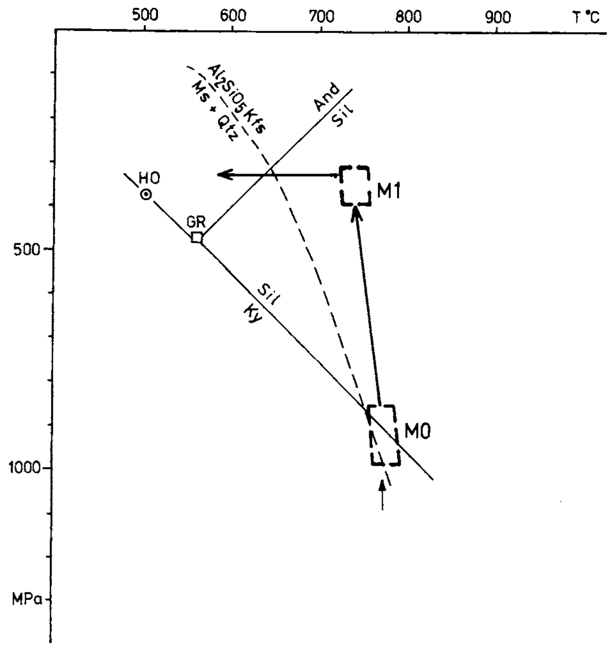


**Fig. 7.** P-T path showing the main metamorphic events M0 and M1 estimated on the basis of thermobarometric calculations and the Grt + Bt + Kfs + Pl + Sil/Ky assmeblage. The $Al_2SiO_5$ triple point after Holdaway (1971, HO) and Greenwood (1976, GR).

Le Breton & Thompson (1989) demonstrated experimentally that in fluid-absent systems the melting begins, through the reaction Bt + Pl + Als + Qtz, at 760 - 800 °C and pressure 1000 MPa, and at 850 °C the melting is extensive. Natural biotites are stable at higher temperatures of the dehydration melting by the increased Ti content. At high pressure dehydration melting of biotite from metapelites the system is closed and the segregation of melt does not occur. The amount of melt depends on the proportion of biotite and muscovite in source metapelites, on the temperature reached and on the amount of $H_2O$ entering the melt (Le Breton & Thompson 1989).

The gneisses and amphibolites of the northern part of the Branisko Mts. contain relics of granoblastites (in the sense of Winkler 1979) having formed by the dehydration anatexis of metapelites at high temperature and pressure conditions. The *in situ* melting is indicated by granoblastic structures with the coarse or fine plagioclase crystals resembling those crystallizing from melt, euhedral shape and rarely indications of oscillatory zoning. A restricted possibility of the melt migration in such extreme P-T conditions is documented by the occurrence of numerous "restites" of Grt - Bt - Sil granoblastites in the migmatite complex.

After the main metamorphic events the crystalline complex got to upper parts of the Earth' crust. The decrease of $P_{total}$ and a possible water influx in the upper crustal parts caused that the anatexis and the following migration of melt occurred at relatively lower temperatures and pressures, as demonstrated by earlier experimental works (Tuttle & Bowen 1958; Winkler & Breitbart 1978). It is indicated by the P-T conditions of higher amphibolite facies recorded at the contacts of garnet rims and biotite. The sequence of individual metamorphic events is hardly possible to date because of lacking radiometric data form this area. It is very probable that the metamorphic events M0 and M1 are related to a single orogen, to its compression and decompression stages. The M2 event may have been connected with the pre-Permian post-orogenic uplift and possible horizontal displacements. It is evidenced by abundant ocurrence of blastomylonite pebbles and cataclastic quartz of banded texture in Permian conglomerates. The possibility of Variscan or pre-Variscan age of the events has to be proved by a further geochronological research. Geologically, the pre-Permian age of the northern Branisko gneiss-amphibolite complex can be unequivocally evidenced (the occurrence of rock fragments in conglomerates of the Korytné Formation - Vozárová & Vozár 1988).

The last cataclatic deformation (M3) is related to the Alpine orogen.

## Conclusions

The petrological analysis of rocks of the northern Branisko gneiss-amphibolite complex has brought the evidence of HT/HP metamorphism relics indicating boundary conditions of the granulite facies.

A relatively broad range of temperatures and pressures (675 - 770 °C, 390 - 630 MPa) was determined in garnet cores by thermobarometric methods. The regressive P-T trend is documented by temperatures and pressures calculated from garnet rims (590 - 680 °C, 260 - 420 MPa, respectively) and by retrograde net transfer reactions represented by Sil + Bt + Qtz and by kyanite to sillimanite transformation. The final stage of the gneiss-amphibolite complex stabilization occurred at temperatures above 550 °C which is documented by the association of Mus + Qtz after Sil + Kfs.

The character of garnet zoning and the almost flat Ca diffusion profile from core to rim suggest a P-T path with an almost isothermal initial uplift followed by isobaric cooling. The presence of kyanite relics indicates initial presures about 1000 MPa at temperatures about 750 °C. The relatively broad range of calculated temperatures and pressures has been caused by complicated exchange reactions in the assemblage Grt + Bt + Sil + Kfs + Qtz + $H_2O$ along the P-T path and by specific conditions when biotite strongly prevails over garnet, the garnet having relatively small size. Progressive and retrogressive P-T path may probably be related to compressional and decompressional stages of the same orogen during which the lower part of crust was uplifted and stabilised at amphibolite facies conditions. The age of these events is constrained by geological data as pre-Permian (rock fragments occurrences in Permian conglomerates). A more precise dating should be proved by radiometric dating.

**Acknowledgments:** I thank Dr. J. Spišiak, Dr. M. Janák, and Prof. M. Suk for valuable comments and constructive discussion.

**Plate 1:** Fig. 1 - gneiss texture with irregularly resorbed garnets. Plane polarized light, magn. 12x. Fig. 2 - a gneiss texture with intensively resorbed garnets (left upper corner). Plane polarized light, magn. 12x. Fig. 3 - intensively resorbed garnet grains. Plane polarized light, magn. 37x. Fig. 4 - assemblage of perthitic orthoclase + sillimanite + biotite + intensively resorbed garnet + quartz. Crossed nicols, magn. 37x. Fig. 5 - kyanite relics in association with biotite, plagioclase and relics of resorbed garnet (left side) and the assemblage of sillimanite + biotite and garnet relics (right side). Plane polarized light, magn. 37x. Fig. 6 - kyanite relics partially replaced by sillimanite. Crossed nicols, magn. 37x. Fig. 7 - kyanite in association with K-feldspar, replaced by sillimanite. Crossed nicols, magn. 74x. Fig. 8 - kyanite in association with K-feldspar and biotite, replaced by sillimanite. The sillimanite partially replaced by muscovite. Crossed nicols, magn. 37x.

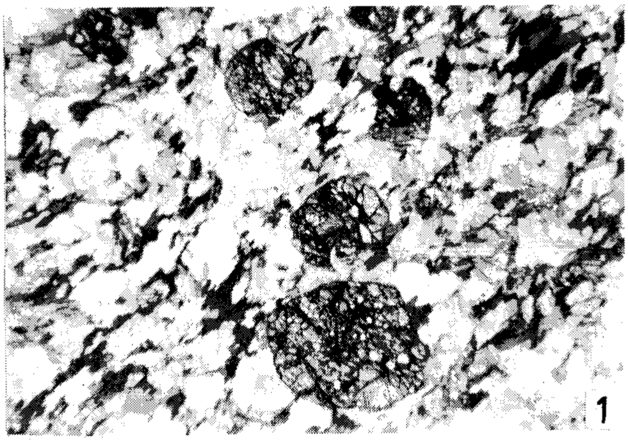
1

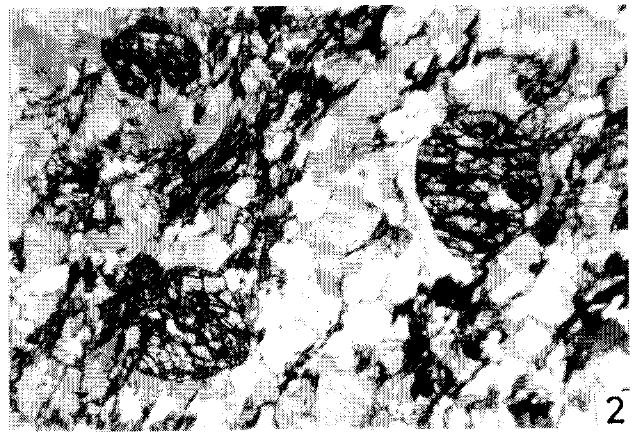
2

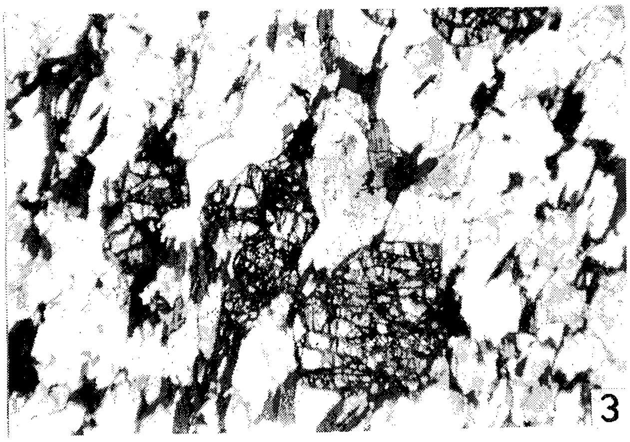
3

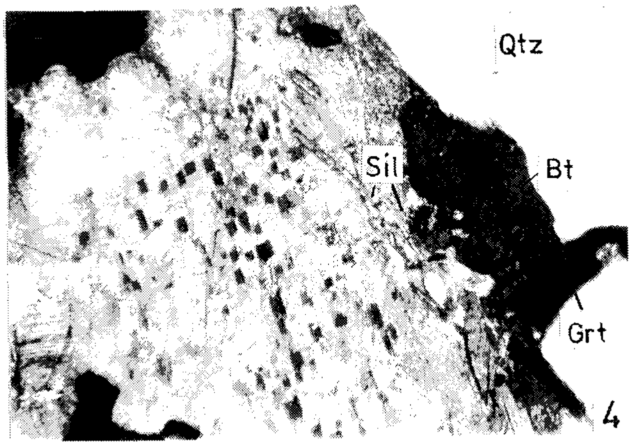
Qtz
Sil
Bt
Grt
4

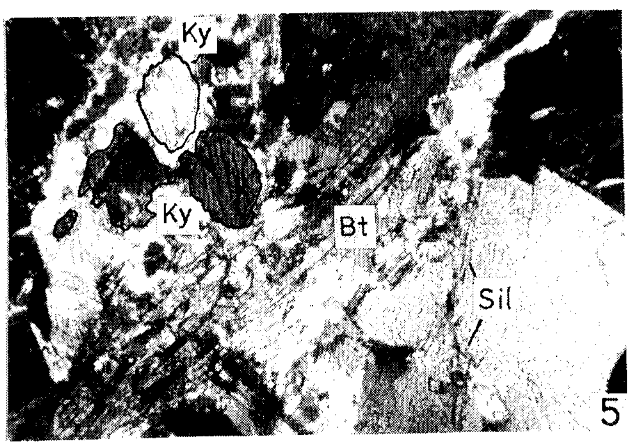
Ky
Ky
Bt
Sil
5

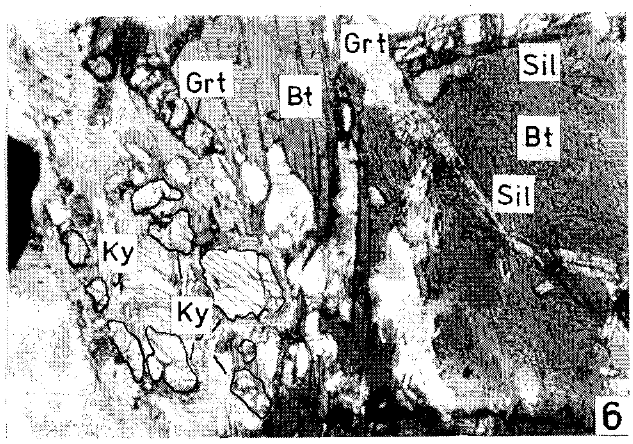
Grt
Grt
Bt
Sil
Bt
Sil
Ky
Ky
6

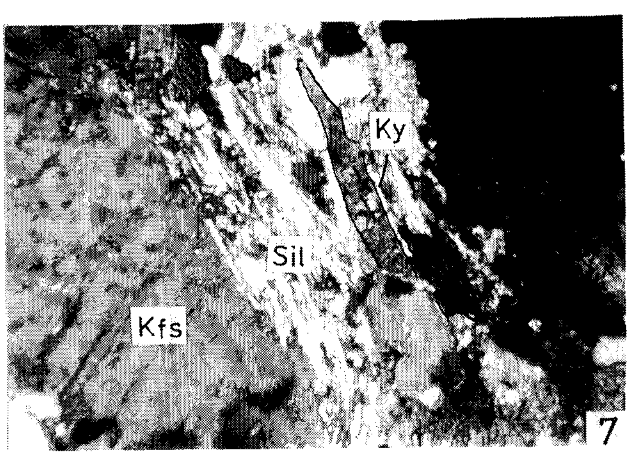
Ky
Sil
Kfs
7


8

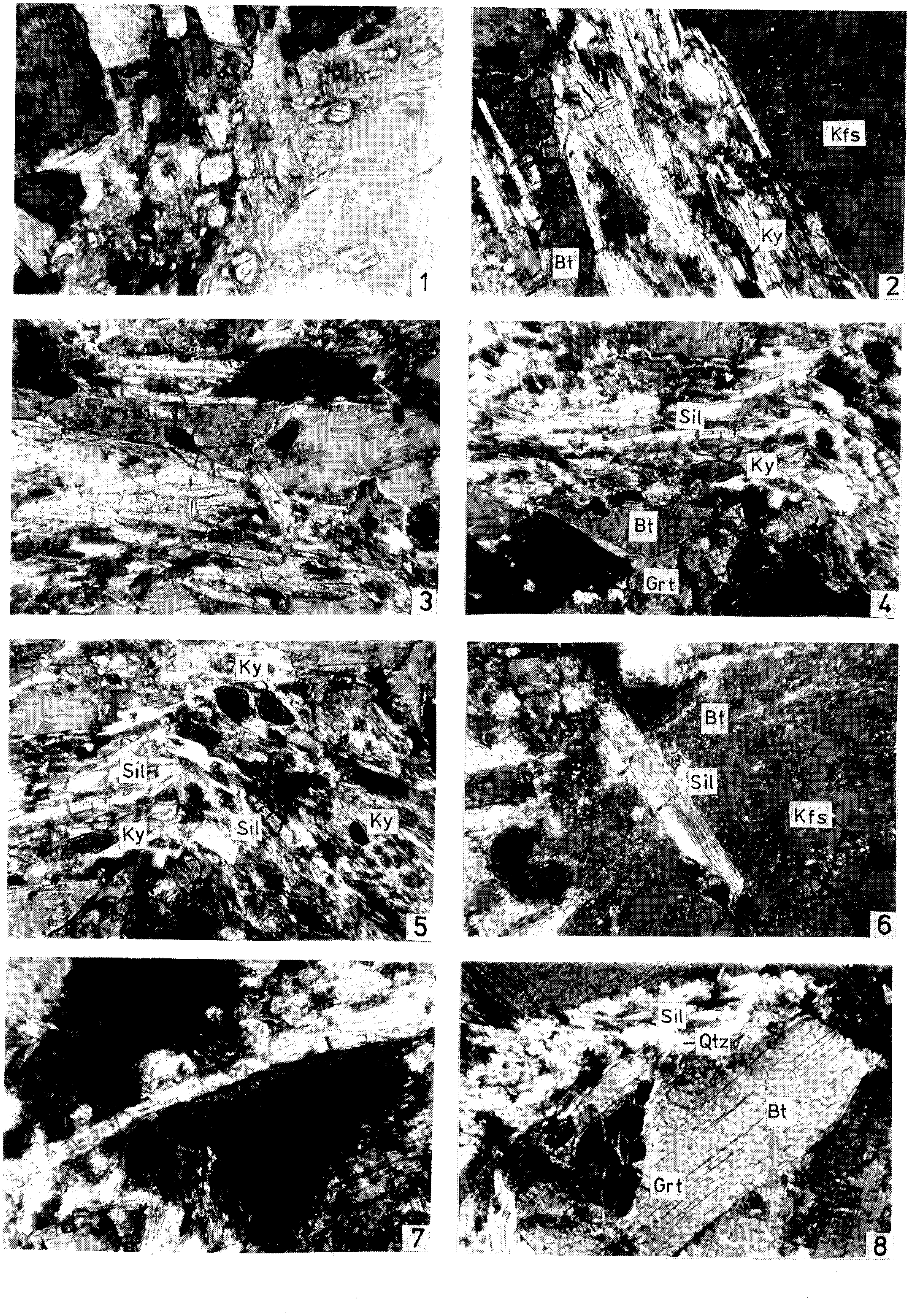
1
Kfs
Ky
Bt
2
3
Sil
Ky
Bt
Grt
4
Ky
Sil
Ky
Sil
Ky
5
Bt
Sil
Kfs
6
7
Sil
Qtz
Bt
Grt
8

## References


Andrusov D., 1958: The geology of the Czechoslovak Carpathians. Vol. 1, *SAV* Publ., Bratislava, 1 - 304 (in Slovak).

Fejdiová O., 1980: The Lúžna sequence - a formal Lower Triassic lithostratigraphic unit. *Geol. Práce, Spr.*, 74, 95 - 101 (in Slovak).

Ferry J. M. & Spear F. S., 1978: Experimental calibration of the partitioning of Fe and Mg between biotite and garnet. *Contr. Mineral. Petrol.*, 66, 113 - 117.

Fusán O., Bystrický J., Franko O., Chmelík F., Ilavský J., Kamenický L., Kulman E., Lukniš M. & Matějka A., 1963: Explanations to the geological map of ČSSR 1:200 000 - Sheet Vysoké Tatry Mts. Geofond, Bratislava, 215 (in Slovak).

Ganguly J. & Saxena S. K., 1984: Mixing properties of alumosilicate garnets: constraints from natural and experimental data and applications to geothermo-barometry. *Amer. Miner.*, 69, 88 - 97.

Goldman D. S. & Albee A. L., 1977: Correlation of Mg/Fe partitioning between garnet and biotite with $^{18}O/^{16}O$ partitioning between quartz and magnetite. *Amer. J. Sci.*, 227, 750 - 767.

Greenwood H. J., 1967: Metamorphism at moderate temperatures and pressures. In: Bailey D. K. & McDonald R. (Eds.): *The evolution of the crystalline rocks. Acad. Press*, London.

Guidotti Ch. V., 1984: Micas in metamorphic rocks. In: Bailey S. W. (Ed.): *Micas. Review in Mineralogy - 13: Book Crafters Inc.* Chelsea, 357 - 468.

Guidotti Ch. V. & Dyar M. D., 1991: Ferric iron in metamorphic biotite and its petrologic and crystallochemical implications. *Amer. Miner.*, 76, 161 - 175.

Hodges K. & Spear F. S., 1982: Geothermometry, geobarometry and $Al_2O_3$ triple point at Mt. Moosilauke, New Hampshire. *Amer. Miner.*, 67, 1118 - 1134.

Holdaway M. J., 1971: Stability of andalusite and the aluminium silicate phase diagram. *Amer. J. Sci.*, 271, 97 - 131.

Holub V. M., Vozár J., Bajaník Š. & Vozárová A., 1981: Geological and paleogeographical map of Carboniferous and Permian in the ČSSR, 1 : 1000 000. *Ústř. Ústav Geol.*, Praha (in Slovak).

Hovorka D., Méres Š. & Krištín J., 1987: Garnets of paragneisses of the Western Carpathian central zone. *Miner. slovaca*, 19, 4, 289 - 309 (in Slovak).

Indares A. & Martignole J., 1985: Biotite-garnet geothermometry in the granulite facies: the influence of Ti and Al in biotite. *Amer. Miner.*, 70, 272 - 278.

Korikovsky S. P., Kahan Š., Putiš M. & Petrík I., 1987a: Metamorphic zoning in the Suchý crystalline complex and high-temperature autometasomatism in peraluminous granites of the Strážovské vrchy Mts. *Geol. Zbor. Geol. carpath.*, 38, 2, 181 - 203 (in Russian).

Korikovsky S. P., Kamenický L., Macek J. & Boronichin V. A., 1987: P-T conditions of metamorphism of the Malá Fatra crystalline schists (in the section of the Mlynský potok creek and its surroundings). *Geol. Zbor. Geol. carpath.*, 38, 4, 409 - 427 (in Russian, English abstract).

Koziol A. M. & Newton R. C., 1988: Redetermination of the anorthite break down reaction and improvement of the plagioclase-garnet-$Al_2SiO_5$-quartz geobarometer. *Amer. Miner.*, 73, 216 - 223.

Le Breton N. & Thompson A. B., 1988: Fluid-absent (dehydratation) melting of biotite in metapelites in the early stages of crustal anatexis. *Contr. Miner. Petrol.*, 99, 226 - 237.

Mahe̍ľ M., 1986: The geological structure of the Czechoslovak Carpathians. The pre-Alpine units. *VEDA* Publ. House of SAS, Bratislava, 1 - 503 (in Slovak).

Mahe̍ľ M., 1988: Regional geology of Czechoslovakia. Part II - The West Carpathians. *Academia*, Praha, 5 - 707.

Méres Š. & Hovorka D., 1989: Metamorphic development of the Suchý, Malá Magura and Malá Fatra Mts. gneisses. *Miner. slovaca*, 203 - 216 (in Slovak).

Newton R. C. & Haselton H. T., 1981: Thermodynamics of the garnet-plagioclase-$Al_2SiO_5$-quartz geobarometer. In: Newton R. C., Navrotsky A. & Wood B. J. (Eds.): *Thermodynamics of minerals and melts. Springer Verl.*, New-York, 131 - 147.

Perchuk L. L., Lavrentieva I. A., Aranovich L. Ya. & Podlesky K. K., 1983: Biotite-garnet-cordierite equilibrium and evolution of metamorphism. *Nauka*, Moskva, 194.

Polák M., 1987: Mesozoic of the northern part of the Branisko Mts. *Geol Práce, Spr.*, 7 - 18 (in Slovak).

Polák M. & Vozár J. et al., 1985: The geological map 1 : 25 000 - Sheet Lipany 4. Arch. of GÚDŠ (Geol. Inst. D. Štúr), Bratislava.

Powell R. & Holland T.J.B., 1988: An internally consistent thermodynamic dataset with uncertainties and correlations: 3. Applications to geobarometry, worked examples and a computer program. *J. Metamophic Geol.*, 6, 173 - 204.

Reinhardt E. W., 1968: Phase relations in cordierite-bearing gneisses from the Ganonoque area, Ontario. *Canad. J. Earth Sci.*, 5, 455 - 482.

Rösing F., 1947: The geology of the Branisko and Čierna Hora Mts. (Carpathians). *Z. Dtsch. geol. Gesell.*, 99, 1 - 39 (in German).

Spear F. S. & Florence F. P., 1992: Thermobarometry in granulites: pitfalls and new approaches Precambrian research. *Elsevier Sci. Publ. B. V.*, Amsterdam, 55, 209 - 241.

Tuttle O. F. & Bowen N. L., 1958: Origin of granite in the light of experimental studies in the system $NaAlSi_3O_8$-$KAlSi_3O_8$-$SiO_2$-$H_2O$. *Mem. Geol. Soc. Amer.*, 74, 153.

Vozárová A. & Krištín J., 1986: Thermodynamic conditions of metamorphism at the contact of Alpine granodiorite in the southern Veporicum and in the northern Branisko crystalline complex. *Miner. slovaca*, 18, 382 - 383 (in Slovak).

Vozárová A. & Vozár J., 1986: Correlation of tectonic units in the Branisko Mts. based on the knowledge of crystalline complex and Upper Paleozoic. *Spr. o výsk., GÚDŠ* (Geol. Inst. of D. Štúr), 21, 21 - 26 (in Slovak).

Vozárová A. & Vozár J., 1988: Late Paleozoic in West Carpathians. *GÚDŠ - Geol. Inst. of D. Štúr*, Bratislava, 314.

Winkler H.G.F., 1979: Petrogenesis if metamorphic rocks. 5th ed. *Springer Verl.*, New York - Berlin, 348.

Winkler H.G.F & Breitbart R., 1978: New aspects of granitic magmas. *Neu Jb. Mineral. Mtsch.*, 463 - 480.


**Plate 2:** Fig. 1 - kyanite replaced by muscovite in association with biotite, K-feldspar and quartz. Crossed nicols, magn. 74x. Fig. 2 - K-feldspar with sillimanite and biotite. Sillimanite after kyanite. Crossed nicols, magn. 74x. Fig. 3 - sillimanite + biotite + quartz. Relics of K-feldspar and garnet (dark grains). Crossed nicols, magn 74x. Fig. 4 - garnet relics amid of an aggregate consisting of sillimanite + biotite + quartz, with kyanite relics. Crossed nicols, magn. 37x. Fig. 5 - aggregate of sillimanite + biotite + quartz, with relics of kyanite. Crossed nicols, magn. 74x. Fig. 6 - sillimanite crystal associated with K-feldspar and biotite. Crossed nicols, magn. 74x. Fig. 7 - sillimanite + biotite. Crossed nicols, magn. 74x. Fig. 8 - resorbed garnet grain amid of biotite and a muscovite + sillimanite + quartz aggregate. Crossed nicols, magn. 37x.